

RECEIVED BY
NASA STI FACILITY
DATE: 10-11-95
DCAF NO. 619800
PROCESSED BY
☒ NASA STI FACILITY
☒ ESA - SDS ☐ AIAA

NAGS-1904

IN-93-CR

65182

P-12

FIREBALLS

Tsvi Piran

Racah Institute for Physics, The Hebrew University, Jerusalem 91904, Israel

NASA-CR-199518

ABSTRACT

The sudden release of copious γ -ray photons into a compact region creates an opaque photon-lepton fireball due to the prolific production of electron-positron pairs. The photons that we observe in the bursts emerge only at the end of the fireball phase after it expanded sufficiently to become optically thin or after it converted its energy to the kinetic energy of relativistic baryons which convert it, in turn, to electromagnetic pulse via the interaction with interstellar matter. It is essential, therefore, to analyze the evolution of a fireball in order to comprehend the observed features of γ -ray bursts. We discuss various aspects of fireball hydrodynamics and the resulting emitted spectra.

1. Introduction - The Inevitability of Fireballs

The recent observation of the BATSE experiment on the COMPTON-GRO observatory have demonstrated, quite convincingly that γ -ray bursts (grbs) originate from cosmological sources^{1,2}. Preliminary evidence for the predicted^{3,4} correlations between the duration the hardness, the strength and the hardness of the bursts^{5,6} supports this conclusion. The correlation suggests, in agreement with an analysis cosmological C/C_{min} distribution⁴ that the weakest bursts originate from distances of $z \approx 1$, corresponding to a release of $E \approx 10^{51}$ ergs (if the emission is isotropic).

The rapid rise time observed in some of the bursts implies that the sources are compact and that in some cases the size of the source R_i is as small as 100km. The copious release of energy within such a small volume results in an initially optically thick system of photons, electrons and positrons which we call a "fireball". The term "fireball" refers here to an opaque radiation - plasma whose initial energy is larger than its rest mass. The initial optical depth in cosmological grbs for $\gamma\gamma \rightarrow e^+e^-$ is⁸:

$$\tau_{\gamma\gamma} = f_g E \sigma_T / R^2 m_e c^2 \approx 10^{19} f_g E_{i,51} R_{i,7}^{-2}, \quad (e1)$$

where $E_{i,51}$ is the initial energy of the burst in units of 10^{51} ergs, $R_{i,7}$ is the radius into which the energy is injected in units of 10^7 cm and f_γ is the fraction of primary photons with energy larger than $2m_e c^2$. Since $\tau_{\gamma\gamma} \gg 1$ the system reaches rapidly thermal equilibrium (regardless of the initial energy injection mechanism) with a temperature: $T = 6.4 E_{i,51}^{1/4} R_{i,7}^{-3/4}$ MeV. At this temperature there is a copious number of $e^+ - e^-$ pairs which in turn contribute to the opacity via Compton scattering.

The huge initial optical depth prevent us from observing directly the radiation released by the source regardless of the specific nature or the source. The observed radiation emerges only after the fireball has expanded significantly and became optically thin. We should divide, therefore, the discussion of cosmological grbs to two parts: the nature of the energy source (in another paper in this

(NASA-CR-199518) FIREBALLS
(Hebrew Univ.) 12 p

N96-17435

Unclass

volume⁸ we discuss the binary neutron star merger model) and the evolution of a fireball (which we address here). The fireball phase determines the observational features of grbs. This can be compared to the situation in stars in which energy is generated in the core but it leaks out through an optically thick envelope and the observed spectrum is determined by the conditions at the photosphere. Similarly the observed grb spectra is determined by the way that fireballs evolve and release their energy.

Before turning to a discussion of the fireball evolution we discuss two recent proposals to avoid fireballs in grbs. The first idea resembles the fireball to some extent as it is based on a relativistic motion of the source. The observed photons are blue shifted to γ -rays because of the relativistic motion of the source. The local temperature is much lower and the fraction f_g of high energy photons at the source is sufficiently small that $\tau_{\gamma\gamma}$ would be less than one and the photons would escape freely (this is the case, for example, in the pure radiation fireball that we discuss later). The opacity of a source with a spectral index α moving toward the observer with a relativistic factor γ is⁹:

$$\tau_{\gamma\gamma} \approx 6.5 \times 10^6 (2\gamma)^{-(2+\alpha)} R_6 A_{12}^{-2} F_{-7} D_{100}^2, \quad (2)$$

where $F = F_{-7} \times 10^{-7} \text{ ergsec}^{-1} \text{ cm}^{-2}$ is the observed flux, $A = 10^{12} \times A_{12} \text{ cm}^2$, is the area of the emitting region and $D = 100 \times D_{100} \text{ kpc}$ is the distance to the source. Even at the galactic halo one requires $\gamma > 30$ for $\alpha = 2$ or $\gamma > 100$ for $\alpha = 1$. This solution raises, therefore, several other problems which are as serious as the problem that it solves: What is the accelerating mechanism that accelerates the grb sources to such a high relativistic velocities? What is the source of the huge kinetic energy required for the bulk motion of such sources?

Alternatively, a fireball will not appear if the energy is released non-electromagnetically and it is converted to photons at significantly larger distance in which eq. 1 yields $\tau_{\gamma\gamma} \ll 1$. This can happen, for example, if the source emits weakly interacting particles which are somehow converted in route to photons. Such a model based on emission of axions by supernova has been recently suggested¹⁰. It does not explain, however, how to reconcile the supernova rate and the grb rate (which differ by a factor of a thousand)? and how can GeV photons¹¹ emerge from such sources?

2. Fireball Evolution - an Overview

Consider, first, a pure radiation fireball. Initially, when the local temperature T is large, the opacity is large due to e^+e^- pairs¹² and the radiation cannot escape freely. The fireball expands and cools and this opacity, τ_p , decreases exponentially with decreasing temperature. At $T_p \approx 20 \text{ KeV}$, $\tau_p \approx 1$, the fireball becomes transparent, the photons escape freely and the fireball phase ends. While the local temperature is T_p the photons are blue shifted roughly to the original temperature due to the relativistic motion of the fireball at that stage. Preliminary calculations^{12,13,14} show that unlike the spectra observed in grbs (see however¹⁵) the spectra emitted from a pure radiation fireball is a blended thermal spectrum.

In addition to radiation and e^+e^- pairs, astrophysical fireballs may also include some baryonic matter which may be injected with the original radiation or may be present in an atmosphere surrounding the initial explosion^{13,16,17}. This affects the fireball in two ways: The electrons associated with this matter

increase the opacity, delaying the escape of radiation. More importantly, the baryons are accelerated with the rest of the fireball and convert part of the radiation energy into bulk kinetic energy.

As a loaded fireball with a baryonic mass, M , evolves two important transitions take place. One transition corresponds to the change from optically thick to optically thin conditions. The opacity itself has a contribution from electron-positron pairs as well as electrons associated with the baryons. Initially, when the local temperature T is large, the opacity is dominated by τ_p . However, the matter opacity, τ_b , decreases only as R^{-2} , where R is the radius of the fireball. Generally, at the point where $\tau_p = 1$, τ_b is still > 1 and the final transition to $\tau = 1$ is delayed and occurs at a cooler temperature. The photons escape freely at this stages. The electrons and the baryons are however still coupled to the photons until the mean free path for a Compton scattering of an electron on a photons drop to unity. This happens at a slightly larger radius.

The second transition corresponds to the switch from radiation dominated to matter dominated conditions, i.e from $\eta > 1$ to $\eta < 1$, where $\eta \equiv E/Mc^2$, the ratio of the radiation energy E to the rest energy M . In the early radiation dominated stages when $\eta > 1$, the fluid accelerates in the process of expansion, reaching relativistic velocities and large Lorentz factors. The kinetic energy too increases proportionately. However, later when $\eta < 1$, the fireball becomes matter dominated and the kinetic energy is comparable to the total initial energy. The fluid therefore coasts with a constant radial speed. The overall outcome of the evolution of a fireball then depends critically on the value of η when τ reaches unity (or equivalently on whether $R_\eta > R_\tau$ or vice versa). If $\eta > 1$ when $\tau = 1$ most of the energy comes out as high energy radiation, whereas if $\eta < 1$ at this stage most of the energy has already been converted into kinetic energy of the baryons and we have to examine the fate of those extreme relativistic baryons.

The initial ratio of radiation energy to mass, η_i , determines in what order the above transitions take place. Shemi and Piran¹³ identified four regimes:

(i) $\eta_i > \eta_{pair} = (3\sigma_T^2 E_i \sigma T_p^4 / 4\pi m_p^2 c^4 R_i)^{1/2} \approx 10^{10} E_{i,51}^{1/2} R_{i,7}^{-1/2}$ (corresponding to $M < M_{pair} = 5 \times 10^{-13} m_\odot E_{i,51}^{1/2} R_{i,7}^{1/2}$): In this regime the effect of the baryons is negligible and the evolution is of a pure photon-lepton fireball. When the temperature reaches T_p , the pair opacity τ_p drops to 1 and $\tau_b \ll 1$. At this point the fireball is radiation dominated ($\eta > 1$) and so most of the energy escapes as radiation.

(ii) $\eta_{pair} > \eta_i > \eta_b = (3\sigma_T E_i / 8\pi m_p c^2 R_i^2)^{1/3} \approx 10^5 E_{i,51}^{1/3} R_{i,7}^{-2/3}$ (corresponding to $M_{pair} < M < m_b = 5 \times 10^{-8} m_\odot E_{i,51}^{2/3} R_{i,7}^{2/3}$): Here, in the late stages, the opacity is dominated by free electrons associated with the baryons. The comoving temperature therefore decreases far below T_p before τ reaches unity. However, the fireball continues to be radiation dominated as in the previous case, and most of the energy still escapes as radiation.

(iii) $\eta_b > \eta_i > 1$ (corresponding to $M_b < M < 5 \times 10^{-4} m_\odot E_{i,51}$): The fireball becomes matter dominated before it becomes optically thin. Therefore, most of the initial energy is converted into bulk kinetic energy of the baryons, with a final Lorentz factor $\gamma_f \approx \eta_i$.

(iv) $\eta_i < 1$: This is the Newtonian regime. The rest energy exceeds the radiation energy and the expansion never becomes relativistic. This is the situation, for example in supernova explosions in which the energy is deposited into a massive envelope.

3. Extreme Relativistic Scaling Laws

After an initial acceleration phase in which the fireball reaches relativistic velocities and $\gamma \gtrsim \text{few}$ each shell of an extreme relativistic fireball satisfies to order $o(\gamma^{-2})$ the following conservation laws¹⁴:

$$r^2 n \gamma = \text{const.}, \quad r^2 e^{3/4} \gamma = \text{const.}, \quad r^2 (n + 4e/3)^2 = \text{const.}, \quad (3)$$

where n and e are the local baryon and energy densities. These scalings were derived for a homogeneous radiation dominated fireball^{13,12} by noting the analogy with an expanding universe. The same relations are valid, however, for each individual radial shell in the fireball even in the more general inhomogeneous case. These scaling laws also apply to Paczyński's¹⁸ solution for a steady state relativistic wind. They are valid even for fractions of individual shells provided that some general conditions on the angular motion are satisfied.

Eqs. 3 yields a scaling solution which is valid everywhere provided that $\gamma \gtrsim \text{few}$. Let t_0 be the time and r_0 be the radius at which a fluid shell in the fireball first becomes ultra-relativistic, with $\gamma \gtrsim \text{few}$. Label various properties of the shell at this time by a subscript 0, e.g. γ_0 , n_0 , e_0 , and $\eta_0 = e_0/n_0$. Defining the auxiliary quantity D , where

$$\frac{1}{D} \equiv \frac{\gamma_0}{\gamma} + \frac{3\gamma_0}{4\eta_0\gamma} - \frac{3}{4\eta_0}, \quad (4)$$

we find that

$$r = r_0 D^{3/2} (\gamma_0/\gamma)^{1/2}, \quad n = n_0 D^{-3}, \quad e = e_0 D^{-4}, \quad \eta = \eta_0 D^{-1}. \quad (5)$$

These are parametric relations which give r , n , e , and η of each fluid shell at any time in terms of the γ of the shell at that time. The relation for r in terms of γ is a cubic equation. This can in principle be inverted to yield $\gamma(r)$, and thereby n , e , and η may also be expressed in terms of r .

The parametric solution 5 describes both the radiation-dominated and matter-dominated phases of the fireball within the frozen pulse approximation. For $\gamma \ll \eta_0 \gamma_0$, the first term in eq. 4 dominates and we find $D \propto r$, $\gamma \propto r$, which yields the radiation-dominated scalings of eqs. e7. This regime extends out to a radius $r \sim \eta_0 r_0$. At larger radii, the first and last terms in eq. 4 become comparable and γ tends to its asymptotic value of $\gamma_f = (4\eta_0/3 + 1)\gamma_0$. This is the matter dominated regime. (The transition occurs when $4e/3 = n$, which happens when $\gamma = \gamma_f/2$.) In this regime, $D \propto r^{2/3}$, leading to the matter dominated scalings laws (eqs. 10).

It is unlikely that a realistic fireball will be spherically symmetric. In fact strong deviation from spherical symmetry are expected in the most promising neutron star merger model, in which the radiation is expected to emerge through funnels along the rotation axis⁸. The initial motion of the fireball might be fairly complex but once $\gamma \gg 1$ and provided that some simple conditions are satisfied then the motion of each fluid element decouples from the motion of its neighbors and it can be described by the same asymptotic solution, as if it is a part of a spherical shell. We define the spread angle α as $u^r \equiv u \cos \alpha$ and the angular range over which different quantities vary as $\Delta\theta$. Eqs. 3 hold locally if:

$$\alpha < \Delta\theta \quad \text{and} \quad (\alpha < 1/\gamma \quad \text{or} \quad 1/\gamma < \alpha \ll 1). \quad (6)$$

4. Physical Conditions in the Fireball

4.i Radiation-Dominated Phase

The fireball is initially radiation-dominated. During this phase ($e \gg n$) and:

$$\gamma \propto r, \quad n \propto r^{-3}, \quad e \propto r^{-4}, \quad T_{obs} \sim \text{constant}, \quad (7)$$

where $T_{obs} \propto \gamma e^{1/4}$ is the temperature of the radiation as seen by an observer at infinity. (Strictly, the radiation temperature depends on e_r , the energy density of the photon field alone; for $T \ll m_e c^2$, $e_r = e$, but for $T > m_e c^2$, e contains an additional contribution from the electron positron pairs¹³ we neglect this complication for simplicity). The scalings of n and e given in eqs. 7 correspond to those of a fluid expanding uniformly in the comoving frame. Although the fluid is approximately homogeneous in its own frame, because of Lorentz contraction it appears as a narrow shell in the observer frame, with a radial width given by:

$$\Delta R \sim R/\gamma \sim \text{constant} \sim R_i. \quad (8)$$

We interpret eq. 7 and the constancy of the radial width Δr in the observer frame to mean that the fireball behaves like a pulse of energy with a frozen radial profile, accelerating outward at almost the speed of light.

If there are no baryons this phase last until the local temperature drops to T_p and the fireball becomes optically thin. Preliminary calculations^{12,13,14} show that unlike the spectra observed in grbs (see however¹⁵) the spectra emitted at this stage is a blended thermal spectrum.

If baryons are present the radiation dominated phase lasts from the initial size, R_i , until $\gamma = \eta$ at R_η

$$R_\eta = 2R_i\eta = 2 \times 10^{11} \text{ cm } R_{i,7}\eta_4, \quad (9)$$

where the initial thermal energy is converted to the kinetic energy of the baryons:

4.ii Matter-Dominated Phase

In the alternate matter-dominated regime ($e \ll n$), we obtain from eq. 3 the following different set of scalings,

$$\gamma \rightarrow \text{constant}, \quad n \propto r^{-2}, \quad e \propto r^{-8/3}, \quad T_{obs} \propto r^{-2/3}. \quad (10)$$

The modified scalings of n and e arise because the fireball now moves with a constant radial width in the comoving frame. (The steeper fall-off of e with r is because of the work done by the radiation through tangential expansion.) Moreover, since $e \ll n$, the radiation has no important dynamical effect on the motion and produces no significant radial acceleration. Therefore, γ remains constant on streamlines and the fluid coasts with a constant asymptotic radial velocity. The width of the fireball remains constant with:

$$\Delta R = R_i. \quad (11)$$

Eventually, as the particle density decreases this phase ends when the electrons decouple from the photons at R_c :

$$R_c = (a^{1/8}/k^{1/2})\sigma_T^{1/2}(4\pi/3)^{-3/8}E_i^{3/8}R_i^{3/8} = 1.6 \times 10^{15} \text{ cm } E_{i,51}^{3/8}R_{i,7}^{3/8}. \quad (12)$$

4.iii Free Coasting

At very late times in the matter-dominated phase the frozen pulse approximation breaks down. At $R \approx R_c$ the electrons decouple from the photons and at $R > R_c$ the baryons, electrons and photons coast freely. The spread in the Lorentz factor of the baryons leads to a spreading of the fireball whose width becomes:

$$\Delta R = R_i + R/\gamma^2 = 10^7 (R_{i,7} + R_{15}/\eta_4^2) \quad (13)$$

The second term, that expresses the additional spreading, is comparable to the original width at

$$R_w \approx \eta^2 R_i \approx 10^{15} \text{ cm } \eta_4^2 R_{i,7} \quad (14)$$

However if $R_w < R_c$ the spreading does not begin until $R = R_c$.

$$\Delta R \approx \begin{cases} R/\eta^2 \approx 10^7 \text{ cm } R_{15} \eta_4^{-2} & \text{for } R > R_w \text{ and } R > R_c \\ R_i = 10^7 \text{ cm } R_{i,7} & \text{otherwise} \end{cases} \quad (15)$$

5. Interaction of the Fireball with the ISM

Mészáros, and Rees^{19,20} suggested that the interaction between the ultra-relativistic baryons and the interstellar matter (ISM) provides a way to convert back the kinetic energy of the baryons to electromagnetic energy. The situation is similar to the one in supernova remnants (SNRs) in which the kinetic energy of the ejecta is converted to radio emission due to interaction with the ISM. The mean free path of a relativistic baryon in the ISM is $\gtrsim 10^{26} \text{ cm}$, hence the interaction between the baryons and the ISM cannot be collisional. However, from the existence of SNRs we can infer that a collisionless shock can form (possibly via magnetic interaction).

The interaction becomes significant at R_γ where the fireball sweeps an external mass of $M_0/\gamma_F = (E_i/\eta c^2)/\gamma_F$ and loses half of its initial momentum:

$$R_\gamma = \left[\frac{M_0}{(4\pi/3)n\gamma_F} \right]^{1/3} = 1.3 \times 10^{15} \text{ cm } E_{i,51}^{1/3} \eta_4^{-2/3} n^{-1/3} \quad (16)$$

Because of a numerical coincidence $R_w \approx R_\gamma \approx R_c$ for our canonical parameters. R_c is independent of η while R_w increases with η and R_γ decreases with η . Therefore, $R_\gamma < R_c < R_w$ for $\eta > 10^4$ and $R_w < R_c < R_\gamma$ for $\eta < 10^4$.

Just like in SNRs the interaction between the fireball and the ISM produces a forward moving shock, which propagates into the interstellar matter, and a reversed shock propagating into the fireball (see Fig. 2). Following Katz²¹ we denote as region 1 the interstellar matter, $n_1 = n$ and $e_1 \ll n_1 mc^2$. Regions 2 and 3 describe the shocked material. Pressure equilibrium along the contact discontinuity between 2 and 3 requires $e = e_2 = e_3$. Region 4 denotes the fireball where $n_4 mc^2 \gg e_4$.

A critical parameter is f , the ratio of densities (in the local fluid's frame) between region 4 (the fireball's material) and region 1 (the external matter):

$$f = \frac{n_4}{n_1} = \frac{M}{[(4\pi)R^2 \Delta R \gamma] n_1} = \frac{1}{3} \left(\frac{R_\gamma}{R} \right)^2 \left(\frac{R_\gamma}{\Delta R} \right) \approx \quad (17)$$

$$\approx \begin{cases} 5 \times 10^7 E_{i,51} \eta_4 n^{-1} R_{15}^{-3} & \text{for } R > R_w \text{ and } R > R_c \\ 5 \times 10^7 E_{i,51} \eta_4^{-1} n^{-1} R_{i,7}^{-1} R_{15}^{-2} & \text{otherwise} \end{cases}$$

where R_{15} is the radius in units of 10^{15} cm.

The shock conditions between 1 and 2 yield^{22,23}:

$$\gamma_{1,2} = 0.5 \sqrt{e/n_1 m_p c^2} \quad ; \quad n_2 = 4\gamma_{1,2} n_1, \quad ; \quad e \equiv e_2 = \gamma_{1,2} n_2 m c^2 \quad (18)$$

where $\gamma_{1,2}$ is the Lorentz factor of the motion of the shocked fluid relative to the rest frame of an external observer.

The Lorentz factor of the shock front itself is $\sqrt{2}\gamma_{1,2}$. Similar relations hold for the reverse shock (with 3,4 replacing 1,2). The definition of f yields: $\gamma_{3,4} = f^{-1/2} \gamma_{1,2}$ and $n_3 = f^{1/2} n_2$. Using this we can express $\gamma_{1,2}$ and $\gamma_{3,4}$ in terms of γ_F :

$$\gamma_{1,2} = f^{1/4} \gamma_F^{1/2} / \sqrt{2} \quad ; \quad \gamma_{3,4} = f^{-1/4} \gamma_F^{1/2} / \sqrt{2}. \quad (19)$$

This holds if $f < \gamma_F^2 \approx \eta^2$. Otherwise the reverse shock is not relativistic and:

$$\gamma_{1,2} \approx \gamma_F \quad ; \quad \gamma_{3,4} \approx 1. \quad (20)$$

Since f decreases with R the reverse shock is initially non relativistic. Using eq. 17 we find that $f(R_\gamma) < \eta^2$ only if $R_w > R_\gamma$. In this case $f(R_\gamma) \approx (\eta^2/3)(R_\gamma/R_w)$ and a mildly relativistic reverse shock develops, with $\gamma_{3,4}(R_\gamma) \approx (R_w/R_\gamma)^{1/4}$. If $R_\gamma > R_w$ and $R_\gamma > R_c$, $f = \eta^2/3$ at R_γ . f decreased with R and one might expect that a relativistic reverse shock will develop latter. The reverse shock reaches, however, the inner boundary of the fireball shell when the fireball reaches R_γ and a rarefaction wave begins to move forwards from the back of the fireball before a relativistic reverse shock develops.

6. Energy Generation via Synchrotron Cooling

The kinetic energy of the fireball is converted to thermal energy at the shocks. This happens in an optically thin region and the resulting photons can escape and produce the observed grbs. The most likely mechanism for the conversion of the thermal energy to kinetic energy is via synchrotron cooling of the ultra-relativistic electrons. This mechanisms requires a strong coupling between the electrons, which radiate the energy, and the protons, that carry the kinetic energy. It also requires a strong magnetic field. Mészáros and Rees²⁴ discuss various emission mechanisms from the shocks. We discuss here an example of the simplest model.

We assume equipartition between the magnetic and the thermal energies. Using eq. 18 we find:

$$B = .5 \text{Gauss} \gamma_{1,2} n_1^{1/2} \quad \text{and} \quad \epsilon_L = 10^{-8} eV \gamma_{1,2} n^{1/2}, \quad (21)$$

where ϵ_L is the corresponding Larmour energy. Assuming equipartition between the kinetic energy of the shocked electrons and the shocked protons the typical

Lorentz factor of the electrons is larger by (m_p/m_e) then the Lorentz factor of the protons. The typical energy of an emitted photon is $\epsilon_{synch} = (m_p/m_e)^2 \gamma_{1,2}^2 \epsilon_l$. This is blue shifted by another factor of $\gamma_{1,2}$ for an observer at rest. Thus:

$$\epsilon_o \approx 4 \times 10^{-2} eV \gamma_{1,2}^4 n_1^{1/2} \approx \begin{cases} 2 \times 10^4 \text{MeV} f_4 \eta_4^2 n_1^{1/2} & \text{relativistic reverse shock} \\ 2 \times 10^8 \text{MeV} \eta_4^4 n_1^{1/2} & \text{otherwise} \end{cases} \quad (22)$$

Similarly, the typical energy of a synchrotron photon emitted by the reverse shock is:

$$\epsilon_{o,rs} \approx 4 \times 10^{-2} eV \gamma_{1,2}^2 \gamma_{3,4}^2 n_1^{1/2} \approx 2 \text{MeV} \eta_4^2 n_1^{1/2} \quad (23)$$

Interestingly enough this is in the right energy range regardless of the question whether the reverse shock is relativistic or not. This suggests that the observed radiation might come from the reverse shock and demonstrates the potential of this mechanism. However it also shows the difficulty that this mechanism poses. Eqs. 22 and 23 depend on a relatively high power of η . For our canonical parameters the radiation from the reverse shock is in the γ -ray range. The load parameter, η can, however, vary easily by orders of magnitude from one burst to another. It is possible that similar processes produce x-ray bursts, uv-bursts as well as bursts with much harder γ -rays. Alternatively, it is possible that the situation is much more subtle and either η is relatively constant or other mechanisms control the emission. In either it is not clear yet why does the energy emerge in soft γ -rays and the resolution of this puzzle might provide the clue to the enigma of grbs.

7. Beaming and Timing

The emitting source is moving relativistically towards the observer and the observed photons are blue shifted both in a pure radiation fireball, that releases its photons when it becomes optically thin, or in a loaded fireball that emits a grb when it interacts with the ISM. Thus, each observer detects blue shifted radiation from a narrow angle $\approx 1/\gamma$. This does not mean, however, that the overall grb is beamed in such a narrow angle. The overall angular spread depends on the width of the emitting region which depends on the source model (in principle the emission could be over 4π if the fireball is spherically symmetric) and is independent of γ .

The duration of the burst depends on several factors. The original duration of the pulse is $R_i/c \approx 10^{-3} R_{i,7}$. This time scale increases due to spreading of the pulse (which takes place in the free coasting phase) and could be as long as:

$$\Delta T_1 \approx 1.5 \times 10^{-3} \text{sec} E_{i,51}^{1/3} \eta_4^{-8/3} n^{-1/3} \quad (24)$$

for a loaded fireball with $R > R_w$ and $R > R_c$. The duration also increases due to the small angular spread of the signal. A given observer will detect radiation from an angular scale $1/\gamma$ around his line of sight. This will lead to a typical duration of²¹:

$$\Delta T_2 \approx R_\gamma/\gamma_F c = 5 \text{ sec} E_{i,51}^{1/3} \eta_4^{-5/3} n^{-1/3}. \quad (25)$$

The relatively strong dependence of η is an advantage here, as it provides a possible explanation to the large variability in durations of grbs. Clearly ΔT is the longer of ΔT_1 and ΔT_2 .

8. Conclusions

We have shown that fireballs with a large initial ratio η_i of radiation energy to rest mass energy show certain common global features during their expansion and evolution. After a short initial acceleration phase, the fluid reaches relativistic velocities, and the energy and mass become concentrated in a radial pulse whose shape remains frozen in the subsequent expansion. The motion is then described by an asymptotic solution (eqs 7, 10), which gives for each individual shell scaling laws similar to those of a homogeneous sphere.

The expanding fireball has two basic phases: a radiation dominated phase and a matter dominated phase. Initially, during the radiation dominated phase the fluid accelerates with $\gamma \propto r$ for each Lagrangian shell. The fireball is roughly homogeneous in its local rest frame but due to the Lorentz contraction its width in the observer frame is $\Delta r \approx R_i$, the initial size of the fireball. Ultimately, a transition takes place to the matter dominated phase and all the energy becomes concentrated in the kinetic energy of the matter, and the matter coasts asymptotically with a final Lorentz factor $\gamma_F \approx \eta$. The matter dominated phase is itself further divided into two sub-phases. At first, there is a frozen-coasting phase in which the fireball expands as a shell of fixed radial width in its own local frame, with a width $\sim \gamma_F R_i \sim \eta_i R_i$. Because of Lorentz contraction the pulse appears to an observer with a width $\Delta r \approx R_i$. Eventually, the spread in γ_F as a function of radius within the fireball results in a spreading of the pulse and the fireball enters the coasting-expanding phase. In this final phase, $\Delta r \approx R_i/\gamma_F^2$, and the observed pulse width increases linearly with the radius from which the radiation is emitted.

The fireball can become optically thin in any of the above phases. Once this happens the system ceases to behave like a fluid, and the radiation moves as a pulse with a constant width, while the baryons enter a coasting phase like the one described above.

For most realistic loads the fireball becomes matter dominated before it becomes optically thin (unless there is some unknown yet mechanism that separates the baryons from the e^+e^- pairs). In this case the observed grb is produced at $R_\gamma \approx 10^{15}$ cm from the source where the kinetic energy of the baryons is converted to thermal energy and γ -rays due to the interaction of the relativistic baryons with the ISM. We have seen that this process leads to the right time scales for grbs and could potentially lead to the right spectrum. However, at present the simple estimates of the spectrum do not necessarily yield signals at the γ -ray range. An explanation of this feature might provide the key to our understanding of fireballs and grbs.

I would like to thank Ramesh Narayan for numerous helpful discussions. This work was supported in part by a BRF grant to the Hebrew University and NASA grant NAGS-1904 to the CFA.

Reference

1. Meegan, C.A., *et. al.*, *Nature*, **355** 143.
2. Meegan, C.A., *et. al.*, this volume.
3. Paczyński, B. 1992, *Nature*, **355**, 521.
4. Piran, T., 1992, *Ap. J.* **L389**, L45.
5. Norris *et. al.*, 1993, this volume.
6. Davis *et. al.*, 1993, this volume.

7. Piran, T. and Shemi, A., 1993, *Ap. J. L.*, **403**, L67.
8. Piran, T., 1993, This volume.
9. Krolik, J.H. and Pier, E.A., 1991, *Ap. J.*, **373**, 277.
10. Leob, A., 1993, this volume.
11. Dingus, B., *et. al.*, 1993, this volume.
12. Goodman, J., 1986, *Ap. J. L.*, **308** L47.
13. Shemi, A. and Piran, T. 1990, *Ap. J. L.* **365**, L55.
14. Piran, T., Shemi, A. and Narayan, R., 1993, *MNRAS.*, **263**, 861.
15. Palmer, D., M., *et. al.*, 1993, this volume.
16. Paczyński, B., 1990. *Ap. J.*, **363**, 218.
17. Cavallo, G., and Rees, M.J. 1978, *MNRAS.*, **183**, 359.
18. Paczyński, B., 1986, *Ap. J. L.*, **308**, L51.
19. Mészáros, P. & Rees, M. J., 1992. *MNRAS.*, **258**, 41p.
20. Mészáros, P. & Rees, M. J., 1992, *Ap. J. L.*, in press.
21. Katz, J. 1993, *Ap. J.* in press.
22. Blandford, R., D., and McKee, C. F., 1976, *Phys. of Fluids*, **19**, 1130.
23. Blandford, R., D., and McKee, C. F., 1976, *MNRAS.*, **180**, 343.
24. Mészáros, P. & Rees, M. J., 1993, this volume.

Figure Captions

- Fig. 1 R_η (solid line), R_w (long dashed line), R_c (dotted line), and R_γ (short dashed line) as a function of η for $E_i = 10^{51}$ ergs and $R_i = 10^7$ cm.
- Fig. 2 Schematic density profile across the shocks. Region 1 is the interstellar matter. Regions 2 and 3 describe the shocked material, with a contact discontinuity between 2 and 3. Region 4 is the unshocked material of the fireball.

Figure 1

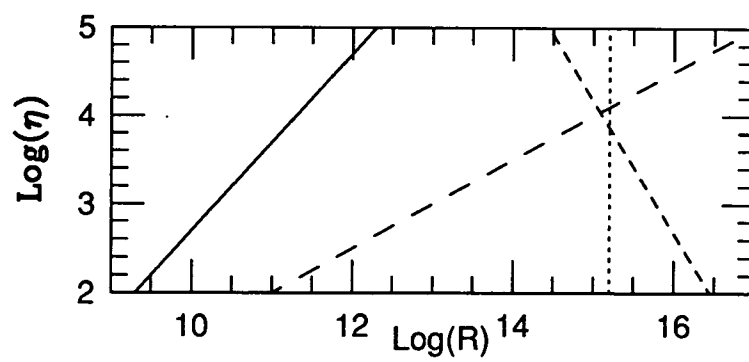


Figure 2

